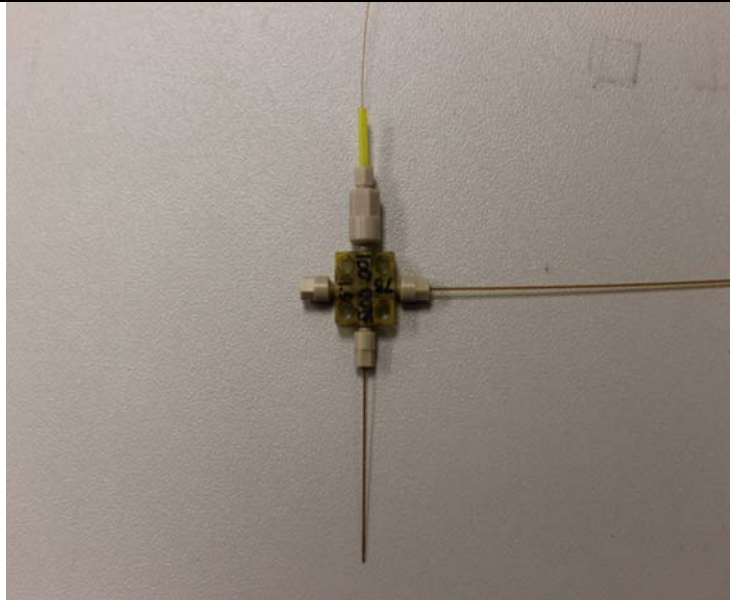


Supplementary Figure 1

A reference image of a capillary not flowing any liquid and with minimal buildup on the outer surface.

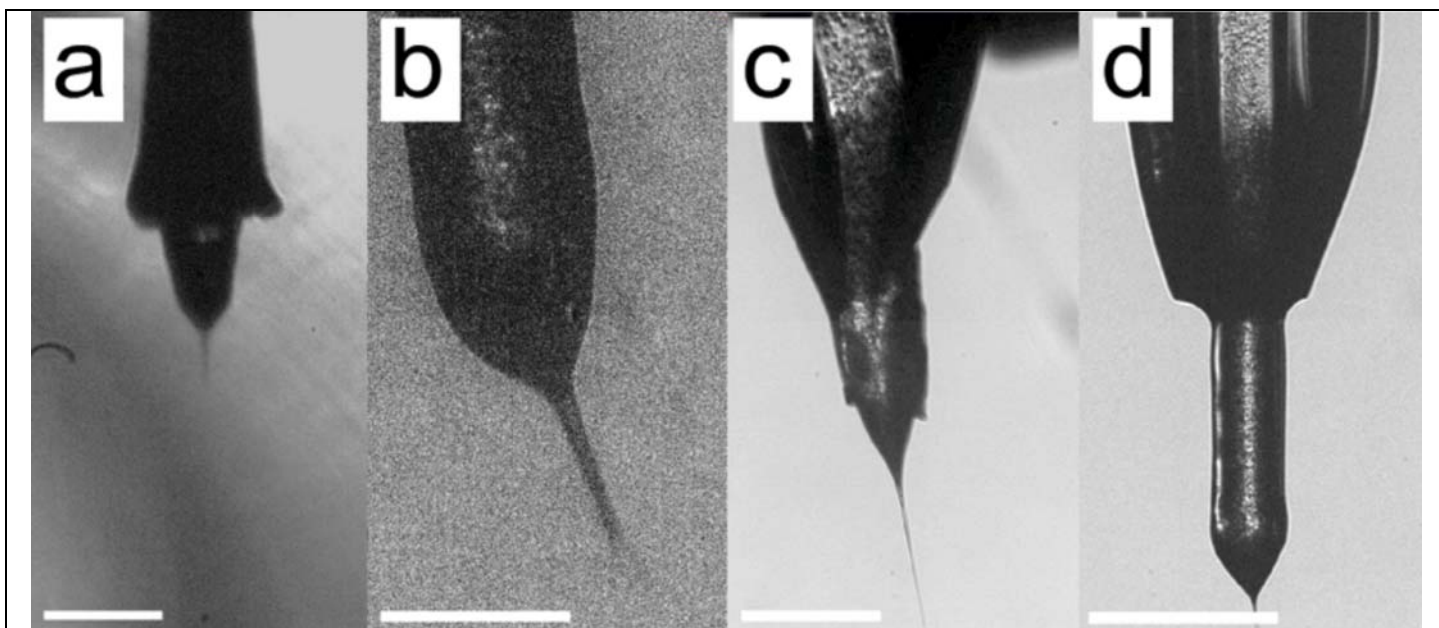
This configuration is typical of the protruded coMESH. The co-terminal MESH would have the smaller inner capillary obstructed from view by the larger outer sheath capillary.



Supplementary Figure 2

A picture of the 360 μm cross fitting used to create the mixing manifold for the coMESH system.

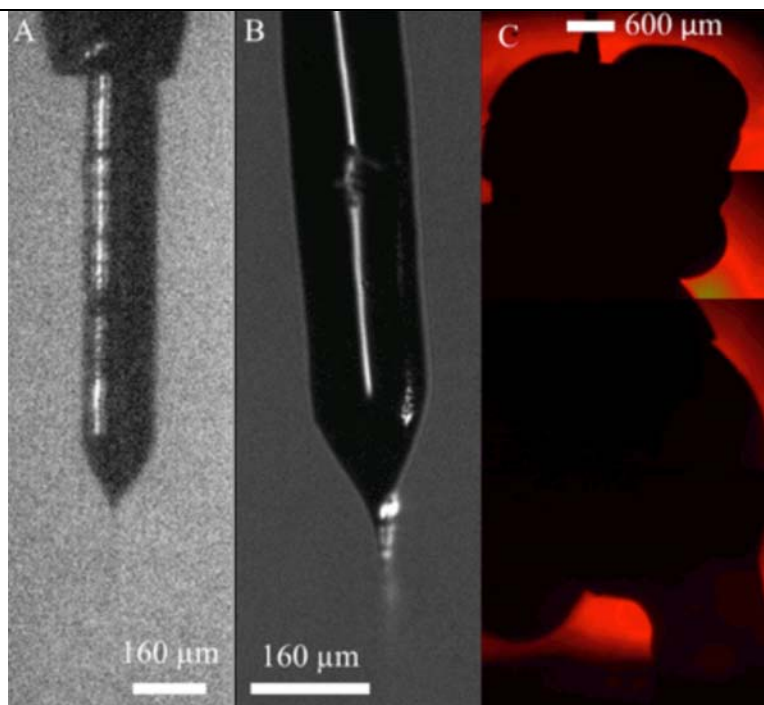
The northern channel contains the 100 μm \times 160 μm \times 1.5 m fused silica capillary, 1/16" (1.6 mm) FEP tubing sleeve, and appropriate 1/16" (1.6 mm) to 360 μm adapter fittings. The capillary passes through the cross and ends at the tip of the south channel seen in the bottom of the figure (not visible, obstructed). Coterminal with the main sample line, is the outer sheath capillary, 200 μm \times 360 μm \times 5 cm, seen in the south. The east line is a 75 μm \times 360 μm \times 1 m capillary and the appropriate 360 μm fitting. The west channel is sealed with a plug fitting.



Supplementary Figure 3

coMESH injection of 30S ribosomal subunit, PSII and thermolysin crystals.

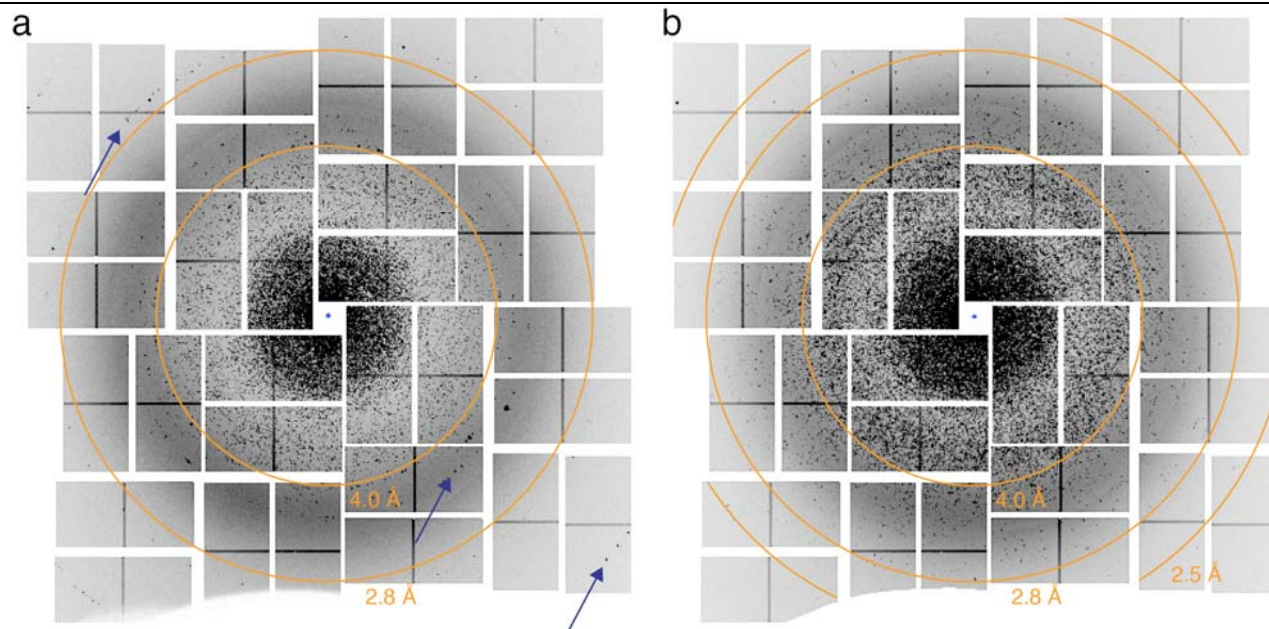
The scale bars in each picture are 360 μm . **(a)** 30S ribosomal subunit crystals: 17% (v/v) MPD mother liquor in 100 μm ID capillary. The sheath flow capillary was a 75 μm ID capillary, and was running 34% (v/v) MPD sister liquor. The outer concentric capillary was 200 μm ID \times 5 cm long tapered fused silica capillary that was coterminal with the inner capillary. The sheath flow was charged by a charging union at 3,000 V and the counter electrode was grounded. The sample ran at 1.5 $\mu\text{l}/\text{min}$ for almost an hour, hence the buildup evident from debris created by the intense X-ray interaction. **(b)** PSII crystals (same capillary conditions as (a)): with the appropriate PSII mother and sister liquor described. Here the sample flow was charged by the syringe reservoir's needle to 7,000 V with the counter electrode at ground. The syringe pump was set to 1 $\mu\text{l}/\text{min}$. **(c)** PSII crystals in modified protruded configuration: Here the flow parameters and geometries are the same as in (b), with the exception that the outer line is simply primed and then capped off and the outer concentric capillary is recessed about 1 mm. **(d)** Thermolysin crystal standard in modified protruded coMESH: similar flow conditions to (c) with samples in 38% (v/v) glycerol, 50 mM CaCl_2 and 0.1M MES. The speckles in the capillary are crystals flowing towards the interaction region.



Supplementary Figure 4

coMESH injection of PSII solution

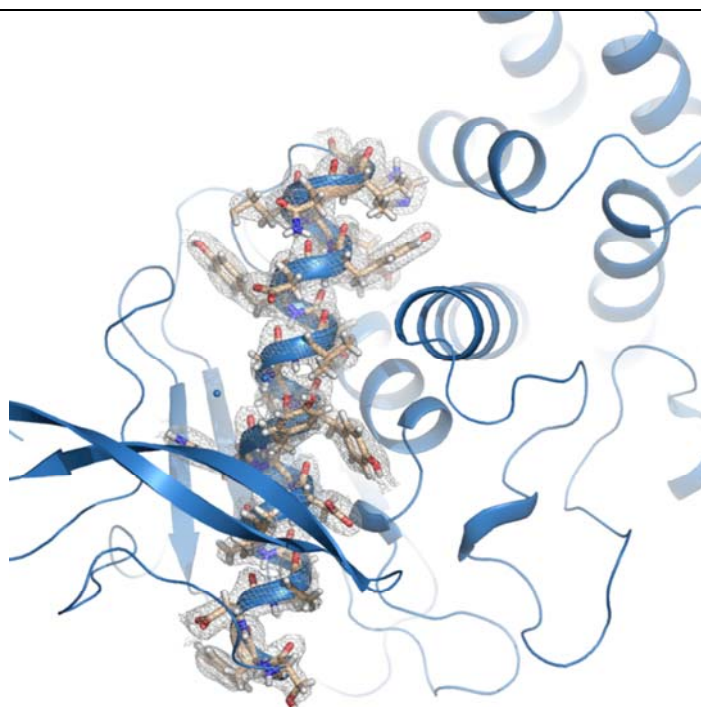
(a) PSII dimer solution (non-crystalline): 6.5 mM chlorophyll, in 40% (v/v) glycerol, 100 μm ID \times 160 μm OD \times 1.5 m long fused silica capillary. The sheath flow capillary was a 30 μm ID \times 150 μm OD \times 1 m fused silica capillary, and was primed with 40% (v/v) glycerol, 0.1 M MES pH 6.5, 5 mM CaCl_2 . After priming, the atmospheric side of the line was capped off. The outer concentric capillary seen in the figure was a 180 μm ID \times 360 μm OD \times 5 cm long, tapered fused silica capillary. The sample flow was charged by the needle of the reservoir syringe and was pushed by a syringe pump set to 2 $\mu\text{l}/\text{min}$. The running voltage was 6,000 V and the counter electrode was grounded. **(b)** A higher resolution image of a PSII solution (non-crystalline) in the protruding coMESH configuration, to emphasize the presence of a wavy irregular appearance at the capillary outer wall, which was possibly a thin coating of liquid from the sheath to aid the meniscus of the sample capillary. **(c)** A picture of an injector failure in a single capillary (top of the figure behind the scale bar) configuration (large black build-up is frozen PEG-solution at the injector tip and red background is from illumination LED). The solution was a high molecular weight PEG solution. This solution failed in a very similar manner when unassisted by a sister liquor in an extended coMESH configuration.



Supplementary Figure 5

Diffraction images of PSII micro crystals measured with two MESH configurations.

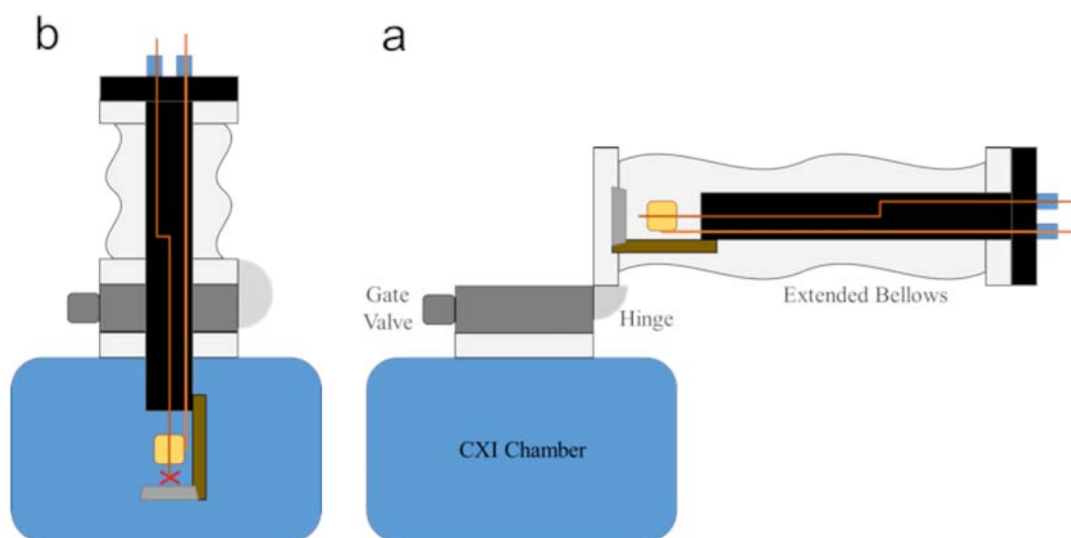
Images are composite powder patterns, showing the maximum pixel values observed over all diffraction events during 9 minute experimental runs for PSII crystals in **(a)** the protruded coMESH configuration aimed to minimize background scatter, however, it created diffraction rings from fluid freezing and precipitation **(b)** the co-terminal coMESH configuration. The crystals were suspended in 0.1 M TRIS, 0.1 M ammonium sulfate, 5% (v/v) ethylene glycol, 35% (w/v) PEG 5000. The sheath flow in (b) was 50% (v/v) ethylene glycol, 50 mM TRIS, and 50 mM ammonium sulfate. In condition (a), using the single-capillary MESH configuration without sheath showed evidence of fluid freezing and precipitation (indicated by blue arrows at 3.47, 2.70 and 2.25 Å). Resolution is indicated by orange rings (4.0 and 2.8 Å(a) and 4.0, 2.8 and 2.5 Å (b)) for reference.



Supplementary Figure 6

Electron density map of thermolysin obtained by using microcrystals injected by coMESH.

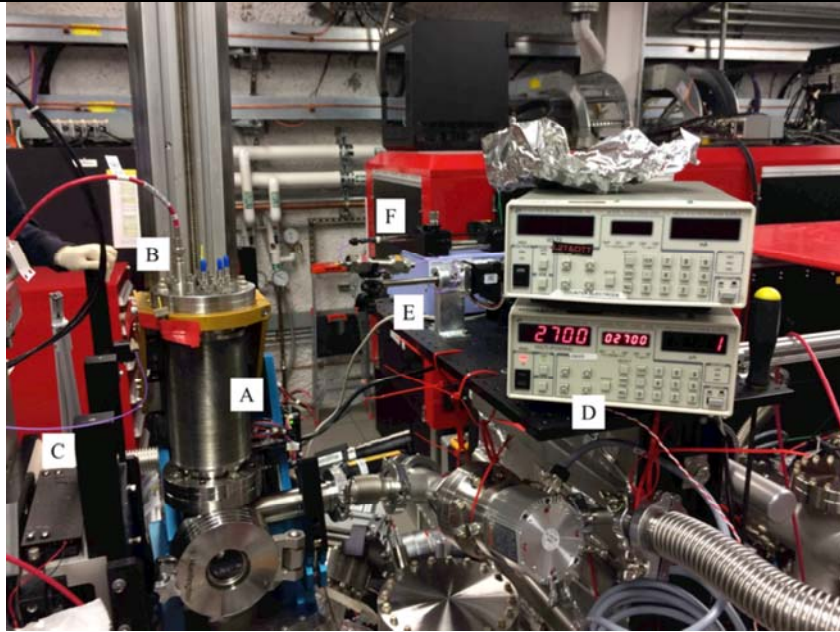
Close-up view of a representative helix structure residues Ser65 (bottom) - His88 (top) with calculated $2F_o - F_c$ electron density map contoured at the 1.0σ level.



Supplementary Figure 7

Schematic of the load lock system used for positioning the injector capillary close to the interaction region.

In its operating position (a) the capillary tip is located close to the interaction region (x) and can be precisely positioned by an XYZ stage (not shown). The coMESH setup is represented by the yellow block with connecting capillary lines that pass through the 6" (15.24 cm) flange out of vacuum. In order to clean or change the capillary the load lock bellows can be extended and after closing the gate valve on top of the experimental chamber, can be tilted by 90° (b) to allow easy access to the injector capillary. The entire injector assembly is comprised of the feedthrough flange and mounting rod (black), the counter electrode (gray trapezoid) and PEEK holder (brown). The assembly is mounted to a 6" (15.24 cm) flange at the top of the load lock bellows and can be easily swapped for a second injector assembly if necessary. The flange has all the necessary feed-throughs for the liquid lines, high voltage connections and three optical fiber feed-throughs for optional *in situ* sample illumination.



Supplementary Figure 8

A photo of the coMESH setup running ribosome crystals at the CXI beamline, prior to receiving X-rays.

On the left, the custom loadlock (A) is mounted on the top of the main CXI ($1 \times 1 \mu\text{m}^2$ beam) sample chamber (not visible); the stick is lowered allowing the coMESH to reach the interaction region. Both capillaries and grounding line are attached to appropriate feedthroughs at the top of the 6" (15.24 cm) flange of the sample stick (B). Not seen is the inline charging fitting connected to the purple polymer tubing (C) feeding the sister liquor. On the right, the high voltage supply (D) is seen in front of the sample rocker (E) holding the custom sample reservoir, with the syringe pump and sister liquor syringe reservoir seen further back (F).

Supplementary Table 1. A table of common injection liquids and their associated failure modes when run on the single-capillary MESH system *in vacuo*, along with an appropriate sister liquor that corrected the problem in a lab setting. Ribosome and PSII crystals were reported in the article. PSI crystal slurry was not run in the lab, however, water was used as a representative condition. Lysozyme crystal slurry was run in a test chamber and not in the CXI chamber, nor in the presence of X-rays. The coMESH format was similar to that described in the Online Methods for the ribosome with the exception of a sample rocker; syringe pumps and glass syringes were used as reservoirs.

Mother Liquor	Common Failure Mode	Typical Crystal Sample	Sister Liquor (stabilizing solution)
Water	freezing	photosystem I	10% (w/v) PEG 2000 30% (v/v) glycerol 5 mM CaCl ₂ 100 mM MES (pH 6.5) -OR- 50% (v/v) MPD 15 mM Magnesium acetate 200 mM Potassium acetate 75 mM Ammonium acetate 100 mM MES (pH 6.5)
35% (w/v) PEG5000 100 mM ammonium sulfate 100 mM TRIS (pH 7.5)	dehydration	photosystem II	50% (v/v) ethylene glycol 50 mM TRIS (pH 7.5) 50 mM ammonium sulfate
14% (v/v) MPD 15 mM Magnesium acetate 200 mM Potassium acetate 75 mM Ammonium acetate 100 mM MES pH 6.5	jet instability	30S ribosomal subunit crystals	34% (v/v) MPD 15 mM Magnesium acetate 200 mM Potassium acetate 75 mM Ammonium acetate 100 mM MES (pH 6.5)
0.4 M Sodium acetate 10% (w/v) NaCl	freezing and salt precipitation	lysozyme	10% (w/v) PEG 2000 30% (v/v) glycerol 5 mM CaCl ₂ 100 mM MES (pH 6.5) -OR- 50% (v/v) MPD 15 mM Magnesium acetate 200 mM Potassium acetate 75 mM Ammonium acetate 100 mM MES (pH 6.5)

Supplementary Table 2. Data collection and refinement statistics

	Paromomycin (XFEL)	Thermolysin
Data collection	PDB ID (5BR8)	PDB ID (5DLH)
Beamline	LCLS (CXI)	LCLS (CXI)
Space group	P4 ₁ 2 ₁ 2	P6 ₁ 22
Cell dimensions		
<i>a</i> , <i>b</i> , <i>c</i> (Å)	401.3, 401.3, 176.4	93.8, 93.8, 132.2
α , β , γ (°)	90, 90, 90	90, 90, 120
Resolution (Å)	52.84-3.40 (3.52-3.40)*	81.23-2.25 (2.33-2.25)*
<i>R</i> _{split}	0.29 (0.87)	0.094 (0.615)
<i>I</i> / σ (<i>I</i>)	3.0 (0.89)	64.9 (2.81)†
Completeness (%)	100.0 (100.0)	99.9 (99.1)
Multiplicity	72.6 (23.8)	347.6 (6.9)
CC*	0.98 (0.70)	0.99 (0.16)
Wilson B Factor (Å ²)	87.92	36.55
Refinement		
Resolution (Å)	52.84-3.40 (3.52-3.40)	81.23-2.25 (2.32-2.25)
No. reflections	195,895 (19,216)	16,903 (1,208)
<i>R</i> _{work} / <i>R</i> _{free}	0.19/0.23 (0.31/0.36)	0.18/0.23 (0.34/0.38)
No. atoms		
Protein	19145	4487
RNA	32504	
Ligand/ion	595	95
<i>B</i> -factors (Å ²)		
Protein	110.3	48.2
RNA	102.8	
Ligand/ion	83.18	43.3
R.m.s. deviations		
Bond lengths (Å)	0.006	0.004
Bond angles (°)	0.859	0.945

*Values in parentheses are for highest-resolution shell.

† Standard deviations reported for thermolysin reflect the propagation of counting statistics only, not the true variance of the structure factor intensity; (Please see Hattne *et al.*, 2014 doi: 10.1038/nmeth.2887).

Supplementary Table 3. Displacement of paromomycin atoms and H-bond distances

16S rRNA residues	16S rRNA H-Bonding atoms	Paromomycin H-bonding atoms	H-bonding distances (Å)	H-Bonding distances (Å)	XFEL vs cryo paromomycin displacements (Å)
			Cryo-cooled	XFEL	
		C11			0.23
		O11			0.23
		C21			0.41
		N21			0.63
		C31			0.44
		O31			0.52
		C41			0.38
A1493	O2P	O41	2.56	2.62	0.48
		C51			0.29
		O51			0.17
		C61			0.39
A1408	N1	O61	2.84	2.76	0.51
		C12			0.57
U1495	O4	N12	2.57	3.05	0.84
		C22			0.54
		C32			0.35
A1493	O1P	N32	3.00	2.59	
G1494	O1P		2.73	2.68	0.56
G1494	N7		2.96	3.27	
		C42			0.11
		C52			0.23
		O52			0.33
		C62			0.46
		O62			0.66
		C13			0.30
		C23			0.88
m5C1407	N4	O23	2.85	3.39	1.40
		C33			0.48
		O33			0.42
		C43			0.33
		O43			0.40
		C53			0.59
G1491	N7	O53	2.75	2.97	0.66
		C14			0.24
		C24			0.58
G1405	O2P	N24	2.92	2.54	0.85
		C34			0.71
		O34			0.70
		C44			0.61
		O44			0.80
		C54			0.23
		O54			0.30
		C64			0.12
C1490	O1P	N64	2.95	3.05	1.32